



High-performance size exclusion chromatography with online fluorescence and multi-wavelength absorbance detection for isolation of high-purity carbon dots fractions, free of non-fluorescent material

Olga Trubetskaya, Oleg Trubetskoj, Alexey Vervalde, Sergey Burikov, Victor Marchenkov, Olga Shenderova, Svetlana Patsaeva, Tatiana Dolenko, Claire Richard

► To cite this version:

Olga Trubetskaya, Oleg Trubetskoj, Alexey Vervalde, Sergey Burikov, Victor Marchenkov, et al.. High-performance size exclusion chromatography with online fluorescence and multi-wavelength absorbance detection for isolation of high-purity carbon dots fractions, free of non-fluorescent material. *Journal of Chromatography A*, 2021, 1650, pp.462251. 10.1016/j.chroma.2021.462251 . hal-03265724

HAL Id: hal-03265724

<https://hal.science/hal-03265724>

Submitted on 22 Jun 2021

HAL is a multi-disciplinary open access archive for the deposit and dissemination of scientific research documents, whether they are published or not. The documents may come from teaching and research institutions in France or abroad, or from public or private research centers.

L'archive ouverte pluridisciplinaire **HAL**, est destinée au dépôt et à la diffusion de documents scientifiques de niveau recherche, publiés ou non, émanant des établissements d'enseignement et de recherche français ou étrangers, des laboratoires publics ou privés.

**High-performance size exclusion chromatography with online fluorescence
and multi-wavelength absorbance detection for isolation of high-purity
carbon dots fractions, free of non-fluorescent material**

Olga E. Trubetskaya^{a,*}, Oleg A. Trubetskoj^b, Claire Richard^{c,d}, Alexey M. Vervald^e, Sergey A. Burikov^e, Victor V. Marchenkov^f, Olga A. Shenderova^g, Svetlana V. Patsaeva^e, Tatiana A. Dolenko^{e,*}

^aBranch of Shemyakin and Ovchinnikov Institute of Bioorganic Chemistry, Russian Academy of Sciences, 6, Prospekt Nauki, 142290 Pushchino, Moscow region, Russia

^bInstitute of Basic Biological Problems, Russian Academy of Sciences, 2, Institutskaya str., 142290 Pushchino, Moscow region, Russia

^cClermont Université, Université Blaise Pascal, Institut de Chimie de Clermont-Ferrand, Equipe Photochimie, BP 10448, F-63000 Clermont-Ferrand, France

^dCNRS, UMR 6296, ICCF, F-63171 Aubiere, France

^eFaculty of Physics, M.V. Lomonosov Moscow State University, 1, bldg.2, Leninskie Gory, 119991 Moscow, Russia

^fInstitute of Protein Research, Russian Academy of Sciences, 4, Institutskaya str., 142290 Pushchino, Moscow region, Russia

^gAdamas Nanotechnologies, Inc., 8100 Brownleigh Dr, Suit 120, Raleigh, NC27617, USA

*corresponding authors.

E-mail addresses: olegi03@yahoo.com (O. E. Trubetskaya, Tel.: +7(4967)73-08-59#3227), olegi03@rambler.ru (O. A. Trubetskoj), claire.richard@uca.fr (C. Richard), alexey.vervald@physics.msu.ru (A. M. Vervald), sergey.burikov@gmail.com (S. A. Burikov), vmarch@rambler.ru (V. V. Marchenkov), oshenderova@adamasnano.com (O. A. Shenderova), spatsaeva@mail.ru (S. V. Patsaeva), tdolenko@lid.phys.msu.ru (T. A. Dolenko, Tel.: +7(495)939-16-53; Fax: +7(495)939-11-04).

ABSTRACT

The carbon dots (CDs) from natural nanographite oxide mixture (NGO-MIX) and from its fraction NGO (3.5-10K) recovered after ultrafiltration and dialysis were analyzed by

3D-excitation/emission matrix and high-performance size exclusion chromatography (HPSEC) combined with online fluorescence and absorbance detections. HPSEC chromatograms obtained simultaneously with absorption within the wavelength range 200-500 nm and fluorescence detection at $\lambda_{exc}/\lambda_{em} = 270/450$ nm/nm showed that NGO-MIX sample is not homogeneous and consist of well resolved CDs fractions with different sizes, absorption spectra and distinct fluorescence and non-fluorescence properties. Despite the twice higher fluorescence intensity of fraction NGO (3.5-10K) compared to the NGO-MIX, some impurity of non-fluorescent components was detected by HPSEC. The absorbance spectra of chromatographic peaks, extracted from the data of multi-wavelength absorbance detector, demonstrated different combinations of absorbance maxima. It means that different chromatographic peaks correspond to sized and chemically different CDs fractions. This study demonstrated for the first time the possibility of separating oxidized nanographite into homogeneous free from non-fluorescent material CDs fractions with their simultaneous spectroscopic characterization.

KEYWORDS: natural nanographite oxide, carbon dots, absorbance, fluorescence, EEM, HPSEC

1. Introduction

At the present time much attention is devoted to carbon dots (CDs), which along with natural biocompatibility demonstrate stable intense fluorescence sensitive to changes in the environment [1]. These properties open up prospects for the utilization of these nanoparticles as optical sensors for various impurities in liquid and gaseous media [2-5], and as theranostic nanocomplexes that simultaneously act as luminescent biomarkers and drug carriers [6-9]. The relevance of using such CDs is primarily associated with the active development of science and technology, where the issue of controlling the content of various substances in multicomponent media, monitoring the occurrence of chemical reactions in various technological processes, and the need to create luminescent medical nano-agents are becoming increasingly acute [10].

The CDs can be synthesized by a variety of physicochemical methods from various carbon-based starting materials [11-14]. In most cases, the end product of CDs synthesis is a complex mixture of compounds with significantly different properties. Unfortunately, at

present, there is no exact way to certify the composition, which significantly complicates the development of a methodology for their application in specific tasks. The major drawback limiting the application of CDs in the life sciences is their not fully understood structure and relatively low quantum yield. Obtaining pure CDs, devoid of various non-fluorescent impurities, should help to reveal their natural chemical structure and provide important insights for understanding the optical properties of CDs synthesized by a strong oxidation process. The isolation of homogeneous fluorescent CDs free of non-fluorescent compounds will significantly increase the quantum yield, sensitivity, and, consequently, the operational efficiency of CD-based nanosensors.

Currently, a number of methods were suggested for CDs separation and purification including electrophoretic techniques, ultrafiltration and dialysis, solvent extraction, density gradient centrifugation or differential centrifugation, reverse phase, and anion exchange high-performance liquid chromatography [15-19]. Due to the fact that most as-prepared CD mixtures contain nanoparticles of different sizes, size-exclusion chromatography (SEC) becomes one of the most promising methods for the task. For this reason, various SEC methods with different combinations of solid and mobile phases including conventional low-pressure size-exclusion chromatography (conventional SEC) [20-25] and high-performance size-exclusion liquid chromatography (HPSEC) [26] have been used previously for purification and fractionation of CDs mixtures. However, detailed size-dependent fluorescence properties of CDs have not been clearly understood and sometimes controversial. Several research groups used preparative conventional SEC on the column with Sephadex G-100 in water as eluent for purification of fluorescent CDs from uncolored reagents in mixtures, prepared from carbon soot by Hammers method and reduced by NaBH_4 [20], passivated by $\text{PEG}_{1500\text{N}}$ [21], doped by ZnS or TiO_2 [22], without online detectors. The fluorescence emission and excitation spectra of CDs mixtures before and after purification were found to be rather similar, while their fluorescence quantum yields increased by several times [20-22]. The CDs mixture, extracted from instant coffee powder, were cleaned without online detectors from uncolored non-fluorescent compounds by conventional SEC on Sephadex G-25 in water and the mixture of CDs of different sizes has been obtained [23].

Arcudi et al. [24] divided the CDs mixture obtained from arginine and ethylenediamine by the microwave method into three fractions based on the elution volumes (V_e) using fractionation on Sephadex LH-20 in methanol as the eluent. However, the authors have shown neither the chromatographic column size nor the V_e of fractions. Therefore, it is not clear if

fractions were eluted from the column due to the size exclusion effect or due to hydrophobic, ionic or other interactions with the solid phase. Kokorina et al. [25] used a ready-made PD-10 desalting column with Sephadex G-25 in water as eluent for fractionation of CDs synthesized from dextran sulfate sodium salt by the hydrothermal method and three fractions with different size were detected offline at V_e more than total column volume (V_t). Some reversible adsorption of analytes on the Sephadex G-25 gel seems to take place. The reason is likely to be the similar dextran nature of Sephadex gel and the source of the CDs mixture that was prepared. Fuyuno et al. [26] used HPSEC on three Cosmosil CNT-columns connected with online absorbance detection for fractionation of graphene CDs mixture and several different average size fractions were collected within the one broad absorption chromatographic peak, eluted after a total column volume of three columns. Typically, as the CD nanoparticles become smaller, the fluorescence energies are blue-shifted to higher energies [27]. However, some blue shift has been observed only in [26] and, on the contrary, the emission maxima of CD fractions increased with decreased nanoparticles size in [25] or were independent on size in [24]. The authors [24] believed that the surface state emission can play a predominant role in the fluorescence properties of CDs, leading to size-independent emission.

Thus, the efficiency of conventional SEC and HPSEC to increase the fluorescence quantum yields of CD mixtures as compared to as-prepared synthesized in various ways was shown. The SEC-separation of CD mixtures into fractions with different sizes and fluorescence properties was shown to be possible as well [24-26], but some questions about the role of adsorption of analyte on the solid phase still needs explanation. In addition, in studies discussed above SEC-experiments have been performed without detectors [20-25] or with an absorbance detector at one wavelength [26], and fractions were collected by color or by V_e with subsequent offline analysis. These approaches do not allow one to be sure that the obtained fluorescent CDs are completely free of non-fluorescent components. Meanwhile, SEC coupling with online simultaneous fluorescence and absorbance measurements may be useful for application to CDs separation; however, we are not aware of any data in the literature about the isolation of CDs by this approach. Additionally, such coupling should be valuable for the understanding of CDs optical properties and could help in clarifying their nature.

In this study, the possibility of isolation of high-purity CDs fractions, free of non-fluorescent material, from natural nanographite oxide by HPSEC combined with online

fluorescence and multi-wavelength absorbance measurements for the first time has been shown.

2. Materials and methods

2.1. Synthesis of NGO-MIX

The CDs mixture was synthesized by the Hammers method from natural nanographite (NG) according to [28]. To this end, 200 mg of NG was added to 50 ml of 95% sulfuric acid (Aldrich) and 68% nitric acid (J.T. Baker) mixture (proportion 3:1) in a 200 ml three-neck round-bottom flask. The NG oxidation was carried out at 130 °C during 150 min. After cooling to room temperature the supernatant was separated from insoluble graphitic residues by centrifugation at 5000 rpm for 10 min, diluted 10 times with distilled water, and neutralized with 1M sodium hydroxide (Fisher). The neutralized CDs mixture, named NGO-MIX was purified from salts on Spectra/Por regenerated cellulose dialysis tubing with molecular weight cut off (MWCO) 1 kDa for three days against distilled water and recovered by drying under vacuum at 50 °C. Ten milligrams of dry NGO-MIX were dissolved in distilled water at a concentration of 2 mg/ml (optical density of about 2.2 at 270 nm) and used as a stock solution for further spectroscopic and HPSEC analyses.

2.2. Separation of fraction NGO (3.5-10K) from the bulk NGO-MIX

Twenty milligrams of dry NGO-MIX were dissolved in 5 ml of distilled water and size separated by centrifugation on Pall filter 10K (MWCO 10kDa). Then the ultrafiltrate with nominal molecular weight (NMW) < 10 kDa was dialyzed in Spectra/Por regenerated cellulose dialysis tubing with MWCO 3.5 kDa for three days against distilled water. The resulting aquatic solution with optical density of about 1.9 at 270 nm containing a part of NGO-MIX with NMW between 10 and 3.5 kDa was named fraction NGO (3.5-10K).

2.3. UV-visible absorption and 3D-fluorescence excitation/emission spectroscopy of NGO-MIX and fraction NGO (3.5-10K)

The UV-visible absorption spectra of aqueous NGO-MIX and its fraction NGO (3.5-10K) were recorded in a 1 cm quartz cuvette using a Cary 3 spectrophotometer (Varian, Cary, USA). The 3D-fluorescence excitation/emission matrix (EEM) of both samples were recorded

using a Cary Eclipse fluorescence spectrophotometer (Varian, Cary, USA) in a 1-cm four-sided quartz cuvette. To minimize the inner filter effect, the solutions were diluted with water to reach an absorbance of 0.05 ± 0.01 at 270 nm. The excitation wavelength range was 200-520 nm and the emission one 250-800 nm. Stepwise increments of 10 and 1 nm were used for excitation and emission wavelengths, respectively.

2.4. High-performance size exclusion chromatography (HPSEC) with online fluorescence and multi-wavelength absorbance detections of NGO-MIX and fraction NGO (3.5-10K)

The HPSEC of NGO-MIX and NGO (3.5-10K) was conducted on a HPLC system with multi-wavelength absorbance detector SPD-M20A (Shimadzu, Japan), operational in the 200-500 nm range. The fluorescence detector RF-20A, connected directly to the line of the absorbance detector, was set to an excitation wavelength 270 nm, emission wavelength 450 nm, and used for measurements of fluorescence emission. The column TSKgel G2000SW_{XL} (7.8 mm ID, 300 mm L, particles size 5.0 μ m, average pore size 12.5 nm) equipped with a guard column (Tosoh Bioscience, Japan) with a fractionation range from 150 to 5 kDa for globular proteins was used. The 30 mM phosphate buffer (pH 6.5) was used as eluent. The flow rate was set to 1.0 ml min⁻¹. The void column volume (V_o) and the permeation volume (V_p) were 5.6 and 13.1 ml, respectively. The solutions of NGO-MIX and NGO (3.5-10K) applied on the column had an absorbance of 1.0 at 270 nm in 30 mM phosphate buffer, and the volume of injection was 0.02 ml. The phosphate buffer used as the mobile phase did not show any absorbance or fluorescence peaks. The entire HPSEC procedure was repeated three times and the deviations did not exceed 3%. The absorbance spectra of chromatographic peaks #1-8 were extracted from the data of the multi-wavelength absorbance detector.

3. Results and Discussion

3.1. Absorbance and 3D-fluorescence spectroscopies of NGO-MIX and fraction NGO (3.5-10K)

The bulk NGO-MIX and its NGO (3.5-10K) fraction, obtained by ultrafiltration and dialysis from the bulk sample, were subjected to UV-visible absorption and 3D-fluorescence excitation/emission analysis. The absorbance spectra of the NGO-MIX sample and fraction NGO (3.5-10K) were found to be quite different. A gradual featureless decrease of absorption

with an increasing wavelength was observed in the NGO-MIX spectrum, while the absorption spectrum of fraction NGO (3.5-10K) had a maximum at 228 nm and a shoulder at 300 nm (Fig. 1a).

The investigation of different fluorescence centers in NGO samples was performed with excitation-emission matrix (EEM) measurements. Unexpectedly, after reviewing the scientific literature, we found that the vast majority of researchers, when studying the fluorescence properties of CDs, used a rather narrow range of excitation wavelengths, usually starting from 300 nm or more to 500 nm [20-25]. Meanwhile, the detection of new emission centers excited by UV light would be undoubtedly useful for both studying CDs structural peculiarities and their practical use. For this reason, the excitation region from 200 to 520 nm with a 10-nm increment was used in our EEM measurements. The EEM spectra were recorded for NGO-MIX and its fraction NGO (3.5-10K) in diluted aqueous solutions with absorbance at 270 nm adjusted to 0.05 to eliminate the inner filter effect and provide an emission intensity proportional to the number of emitting centers (Fig. 1). The NGO-MIX fluorescence spectra exhibited four peaks with the following excitation-emission wavelength maxima pairs ($\lambda_{\text{exc}}/\lambda_{\text{em}}$) 230/440, 240/500, 290/500, and 310/435 nm/nm (Fig. 1b), while the highest emission intensity was found for the pair 230/440 nm/nm. The fraction NGO (3.5-10K) showed similar emission centers, however, the fluorescence intensity of long-wavelength emitting centers ($\lambda_{\text{exc}}/\lambda_{\text{em}}$ 240/500 and 290/500 nm/nm) was much higher than the fluorescence intensity of short-wavelength ones ($\lambda_{\text{exc}}/\lambda_{\text{em}}$ 230/440 and 310/435 nm/nm) (Fig. 1d). The long-wavelength emitting centers seem to be much more concentrated in the fraction NGO (3.5-10K) than in the original NGO-MIX meaning that the essential part of fluorescence centers with short-wavelength emission was lost during the purification procedure of filtering and dialysis. In addition to local centers with high emission, both samples contained low-intensive excitation-dependent long-wavelength emitters (see Fig. 1c and 1e with conventional emission spectra extracted from EEMs). The fluorescence intensity of NGO (3.5-10K) fraction was twice or more higher than the NGO-MIX sample. Thus, the results of the absorption and 3D-fluorescence spectroscopy demonstrated that the original NGO-MIX sample and its fraction NGO (3.5-10K) are not homogeneous and can be split into individual compounds with different fluorescence properties.

3.2. HPSEC with online fluorescence and multi-wavelength absorbance detections of NGO-MIX and fraction NGO (3.5-10K)

To confirm this assumption, we for the first time in the case of CDs used HPSEC with simultaneous fluorescence and multi-wavelength absorbance measurements for separation of NGO-MIX and its fraction NGO (3.5-10K). Taking into account that NGO-MIX CDs nanoparticles sizes are less than 10 nm [28-29], we used column TSKgel G2000SW_{XL} with an average pore size of 12.5 nm to achieve a satisfactory size-separating effect. The 30 mM phosphate buffer (pH 6.5) was used as eluent to suppress the possible over-exclusion effect due to the negative charge of CDs. This approach was successfully used recently for isolation of different in size fluorescent negatively charged compounds from natural dissolved organic carbon of various origins [30-31]. The excitation/emission pair 270/450 nm/nm was set for the fluorescence detector on the basis of the EEM analysis of NGO-MIX and fraction NGO (3.5-10K). At an excitation wavelength of 270 nm the fluorescence intensity of both samples was high and both different emission maxima in NGO-MIX well defined (Fig. 1c). The emission at 450 nm was used to detect all fluorophores emitting in the range 420-550 nm (Fig. 1b,d) during one chromatographic run.

The HPSEC chromatograms of NGO-MIX and NGO (3.5-10K) are presented on Fig. 2. The UV chromatogram of NGO-MIX detected at 210 nm (Fig. 2 a, solid black line) showed four resolved peaks, labeled #1, #3, #6, and #8; the last one on the chromatogram's tailing edge, #8, was considerably more intense than the other ones. On the UV chromatogram with detection at 270 nm (Fig. 2a, dashed black line) the intensities of peaks #1, #3, and #6 were considerably lower and peak #8 was absent. The corresponded chromatogram's fluorescence profile of NGO-MIX at $\lambda_{exc}/\lambda_{em}$ 270/450 nm/nm (Fig. 2a, red line) showed several additional peaks, labeled #1, #2, #4, #5, and #7. The peaks #1-8 were eluted between the void (V_o 5.6 ml) and permeation (V_p 13.1 ml) volumes of the column (Fig. 2a) and no absorbance or fluorescence peaks after V_p were found. This result means that fractionation was based mostly on size differences. The NGO-MIX sample was found to be heterogeneous, consisting of several size-different organic compounds, and only some of them possessed fluorescence properties. It is obvious that the main part of NGO-MIX consists of non-fluorescent compounds focused in peaks #3, #6, and, primarily, #8. The fluorescent compounds (peaks #1, #2, #4, #5, #7) seem to constitute an insignificant part of the bulk NGO-MIX sample. After HPSEC separation of NGO (3.5-10K) the UV chromatogram at 210 nm exhibited peaks #1 and #3 (Fig. 2b, solid black line). The UV chromatogram at 270 nm was similar in shape to that at 210 nm but less intense (Fig. 2b, dashed black line). The fluorescence chromatogram

of NGO (3.5-10K) revealed peaks #1 and #4 (Fig. 2b, red line). In the NGO (3.5-10K) chromatogram the absorbance intensity of peak #3 and fluorescence intensity of peak #4 increased considerably in comparison with peak #1; peaks #2 and #5 were present as shoulders; peaks #6, #7, and #8 were absent. This result could be attributed to the fractionation of NGO-MIX using ultrafiltration and dialysis. The centrifugation on the Pall filter 10K cut off the nanographite oxide portion with NMW more than 10kDa, and during dialysis, the compounds with NMW less than 3.5 kDa were lost. The considerable increase of the fluorescence intensity in about 5 times with the unchanged absorbance of peak #4 in the NGO (3.5-10K) chromatogram in comparison to the NGO-MIX chromatogram showed the essential increase of quantum yield after purification of the NGO (3.5-10K) fraction and thus the higher fluorescence purity of this material. However, in the NGO (3.5-10K) sample some admixture of non-fluorescent matter located in peak #3 was still present.

In the previous SEC-studies, CDs fractions differing in size were collected based on their elution volumes using both visual observation [24-25] and absorbance detection at 254 nm [26] and CDs material has been eluted as one broad peak. This approach does not allow one to show reliably the presence of individual fluorescent or non-fluorescent components in the CDs mixture and to accurately determine their place on the chromatographic profile. Moreover, fractions were collected out of the fractionation range of the column, i.e. after the total column volume [25-26]. Thus, according to the principle of SEC, it is not clear how CDs fractions have been separated according to their sizes or fractions distribution were additionally influenced by interactions (i.g. hydrophobic or ionic) between the gel matrix and fractionated materials. On the other hand, by using our combination of HPSEC-column and mobile phase with simultaneous online fluorescence and absorbance detections, the fractionation of graphene CDs mixture was done based solely on size differences. For the first time several individual monomodal chromatographic peaks were obtained, some of which exhibited fluorescence.

3.3 Comparative analysis of absorbance spectra of bulk NGO-MIX, fraction NGO (3.5-10K), and their HPSEC peaks

The HPSEC with a multi-wavelength absorbance detector operating in the spectral range of 200-500 nm allowed us to get the absorbance spectra of CDs chromophoric fractions

corresponding to each chromatographic peak and to compare them with the absorbance spectra of the bulk NGO-MIX and NGO (3.5-10K) samples (Fig. 3a,b, Table 1).

The UV spectra at λ_{Ve} , corresponding to peak's tops, were extracted from the multi-wavelength absorbance detector data. The absorbance spectra of bulk NGO-MIX and chromatographic peak #8 appeared to be largely similar, the contribution of other chromatographic peaks to NGO-MIX absorbance spectrum was consequential only in the region 230-320 nm (Fig. 2a). After normalization at 200 nm, we found that the absorbance spectrum of peaks #1-#8 demonstrated different combinations of absorbance maxima (Fig. 3a-Inset, Table 1). It means that all different chromatographic peaks correspond not only to differently sized homogenous particles but to chemically different CDs fractions. The bulk NGO (3.5-10K) sample demonstrated the absorbance spectrum with the maximum at 228 nm and shoulder at 300 nm (Fig. 3b, Table 1). The shapes of absorbance spectra of peaks #3 and #4 were more or less similar to that of bulk NGO (3.5-10K) but had more pronounced maxima at 232 nm (peak #3) and 230 nm (peak #4) and different shoulders. The absorbance spectrum of peak #1 was rather different from that of peaks #3 and #4, had a maximum at 221 nm and a shoulder at 270 nm. We attributed the material coming with peaks #1 and #4 as containing different fluorescent CDs fractions. Thus, we achieved the separation of fluorescent CDs with different sizes corresponding to the material in peaks #1, #2, #4, #5, and #7 on NGO-MIX chromatogram and in peaks #1 and #4 on the chromatogram of its fraction NGO (3.5-10K).

4. Conclusions

The NGO-MIX sample and its fraction NGO (3.5-10K) were analyzed for the first time by analytical HPSEC with a combination of online fluorescence and multi-wavelength absorbance detections. It was found that the as-prepared NGO-MIX sample was distributed in eight well-resolved CD fractions with different sizes ranged between 150 to 5 kDa (for globular proteins) and absorption spectra, five of which were fluorescent. In NGO (3.5-10K) sample processed by ultrafiltration and dialysis, the three fractions with the lowest size were removed, decreasing the number of detected fluorescent CDs fractions but also removing the dominant non-fluorescent fraction. Despite the twice higher fluorescence intensity of fraction NGO (3.5-10K) compared to the NGO-MIX sample, some impurity of non-fluorescent components was detected in this fraction by HPSEC. The absorbance spectrum of

chromatographic peaks, extracted from the data of multi-wavelength absorbance detector, demonstrated different combinations of absorbance maxima. It means that different chromatographic peaks correspond to sized and chemically different CDs fractions. Thus, a combination of HPSEC with simultaneous multi-wavelength absorbance and fluorescence measurements allowed the separation and identification of CDs fractions within NGO samples and monitoring of their change upon sample processing. The isolation of CDs free of non-fluorescent material will be useful for obtaining CDs with improved optical properties and sensitivity.

ACKNOWLEDGMENTS

This study has been supported by (1) Russian Foundation for Basic Research (project 19-05-00056a) in part of methodology developing and optical investigation; (2) CNRS-RAS cooperation in part of HPSEC fractionation; (3) Russian Foundation for Basic Research (project 20-32-70150) in part of preparation of NGO-MIX sample and isolation fraction NGO (3.5-10K); (4) funding in framework of state assignment. This research was performed according to the Development program of the Interdisciplinary Scientific and Educational School of Lomonosov Moscow State University «Photonic and Quantum technologies. Digital medicine».

REFERENCES

- [1] J. Fan, P.K. Chu, Group IV nanoparticles: synthesis, properties, and biological applications, *Small*. 6 (2010) 2080–2098. <https://doi.org/10.1002/smll.201000543>.
- [2] M. Yang, H. Li, J. Liu, W. Kong, S. Zhao, C. Li, H. Huang, Y. Liu, Z. Kang, Convenient and sensitive detection of norfloxacin with fluorescent carbon dots, *J. Mater. Chem. B*. 2 (2014) 7964–7970. <https://doi.org/10.1039/c4tb01385a>.
- [3] W. Lu, X. Qin, S. Liu, G. Chang, Y. Zhang, Y. Luo, A.M. Asiri, A.O. Al-Youbi, X. Sun, Economical, green synthesis of fluorescent carbon nanoparticles and their use as probes for sensitive and selective detection of mercury(II) ions, *Anal. Chem.* 84 (2012) 5351–5357. <https://doi.org/10.1021/ac3007939>.
- [4] Y. Guo, Z. Wang, H. Shao, X. Jiang, Hydrothermal synthesis of highly fluorescent carbon nanoparticles from sodium citrate and their use for the detection of mercury ions, *Carbon*. 52 (2013) 583–589. <https://doi.org/10.1016/j.carbon.2012.10.028>.

352 [5] A. Salinas-Castillo, M. Ariza-Avidad, C. Pritz, M. Camprubí-Robles, B. Fernández, M.J.
 353 Ruedas-Rama, A. Megia-Fernández, A. Lapresta-Fernández, F. Santoyo-Gonzalez, A.
 354 Schrott-Fischer, L.F. Capitan-Vallvey, Carbon dots for copper detection with down and up
 355 conversion fluorescent properties as excitation sources, *Chem. Commun.* 49 (2013) 1103–
 356 1105. <https://doi.org/10.1039/c2cc36450f>.

357 [6] P. Miao, K. Han, Y. Tang, B. Wang, T. Lin, W. Cheng, Recent advances in carbon
 358 nanodots: synthesis, properties and biomedical applications, *Nanoscale*. 7 (2015) 1586–1595.
 359 <https://doi.org/10.1039/c4nr05712k>.

360 [7] N. Prabhakar, T. Näreoja, E. von Haartman, D. ŞenKaraman, S.A. Burikov, T.A. Dolenko,
 361 T. Deguchi, V. Mamaeva, P.E. Hänninen, I.I. Vlasov, O.A. Shenderova, J.M. Rosenholm,
 362 Functionalization of graphene oxide nanostructures improves photoluminescence and
 363 facilitates their use as optical probes in preclinical imaging, *Nanoscale*. 7 (2015) 10410–
 364 10420. <https://doi.org/10.1039/c5nr01403d>.

365 [8] O.E. Sarmanova, S.A. Burikov, S.A. Dolenko, I.V. Isaev, K.A. Laptinskiy, N. Prabhakar,
 366 D.Ş. Karaman, J.M. Rosenholm, O.A. Shenderova, T.A. Dolenko, A method for optical
 367 imaging and monitoring of the excretion of fluorescent nanocomposites from the body using
 368 artificial neural networks, *Nanomedicine*. 14 (2018) 1371–1380.
 369 <https://doi.org/10.1016/j.nano.2018.03.009>.

370 [9] E. von Haartman, H. Jiang, A.A. Khomich, J. Zhang, S.A. Burikov, T.A. Dolenko, J.
 371 Ruokolainen, H. Gu, O.A. Shenderova, I.I. Vlasov, J.M. Rosenholm, Core–shell designs of
 372 photoluminescent nanodiamonds with porous silica coatings for bioimaging and drug delivery
 373 I: fabrication, *J. Mater. Chem. B*. 1 (2013) 2358–2366. <https://doi.org/10.1039/c3tb20308e>.

374 [10] B. Yao, H. Huang, Y. Liu, Z. Kang, Carbon dots: a small conundrum, *Trends Chem.* 1
 375 (2019) 235–246. <https://doi.org/10.1016/j.trechm.2019.02.003>.

376 [11] S.-T. Yang, L. Cao, P.G. Luo, F. Lu, X. Wang, H. Wang, M.J. Meziani, Y. Liu, G. Qi,
 377 Y.-P. Sun, Carbon dots for optical imaging in vivo, *J. Am. Chem. Soc.* 131 (2009) 11308–
 378 11309. <https://doi.org/10.1021/ja904843x>.

379 [12] J. Zhong, W. Sun, Q. Wei, X. Qian, H.-M. Cheng, W. Ren, 2018. Efficient and scalable
 380 synthesis of highly aligned and compact two-dimensional nanosheet films with record
 381 performances. *Nat. Commun.* 9, 3484. <https://doi.org/10.1038/s41467-018-05723-2>.

382 [13] H. Li, X. He, Z. Kang, H. Huang, Y. Liu, J. Liu, S. Lian, C.H.A. Tsang, X. Yang, S.-T.
 383 Lee, Water-soluble fluorescent carbon quantum dots and photocatalyst design, *Angew. Chem.*
 384 *Int. Ed.* 49 (2010) 4430–4434. <https://doi.org/10.1002/anie.200906154>.

385 [14] J. Lu, J. Yang, J. Wang, A. Lim, S. Wang, K.P. Loh, One-pot synthesis of fluorescent
 386 carbon nanoribbons, nanoparticles, and graphene by the exfoliation of graphite in ionic
 387 liquids, *ACS Nano*. 3 (2009) 2367–2375. <https://doi.org/10.1021/nn900546b>.

388 [15] A.A. Kokorina, A.V. Sapelkin, G.B. Sukhorukov, I.Yu. Goryacheva, 2019. Luminescent
 389 carbon nanoparticles separation and purification. *Adv. Colloid Interface Sci.* 274, 102043.
 390 <https://doi.org/10.1016/j.cis.2019.102043>.

391 [16] Q. Hu, X. Gong, L. Liu, M.M.F. Choi, 2017. Characterization and analytical separation
 392 of fluorescent carbon nanodots. *J. Nanomater.* 2017, 1804178.
 393 <https://doi.org/10.1155/2017/1804178>.

394 [17] Y. Lu, J. Wang, H. Yuan, D. Xiao, Separation of carbon quantum dots on a C18 column
 395 by binary gradient elution via HPLC, *Anal. Methods*. 20 (2014) 8124–8128. <https://doi.org/10.1039/c4ay01052c>.

397 [18] Q. Hu, M. Chin Pau, Y. Zhang, W. Chan, X. Gong, L. Zhang, M.M.F. Choi, Capillary
 398 electrophoretic study of amine/carboxylic acid-functionalized carbon nanodots. *J.*
 399 *Chromatogr. A*. 1304 (2013) 234–240. <https://doi.org/10.1016/j.chroma.2013.07.035>.

400 [19] Q. Wu, X. Zhang, X. Zhang, S. Dong, H. Qiu, L. Wang, Multi-mode application of
 401 graphene quantum dots bonded silica stationary phase for high performance liquid
 402 chromatography. *J. Chromatogr. A*. 1492 (2017) 61–69.
 403 <https://doi.org/10.1016/j.chroma.2017.02.067>.

404 [20] H. Zheng, Q. Wang, Y. Long, H. Zhang, X. Huang, R. Zhu, Enhancing the luminescence
 405 of carbon dots with a reduction pathway, *Chem. Commun.* 47 (2011) 10650–10652.
 406 <https://doi.org/10.1039/c1cc14741b>.

407 [21] X. Wang, L. Cao, S.-T. Yang, F. Lu, M.J. Meziani, L. Tian, K.W. Sun, M.A. Bloodgood,
 408 Y.-P. Sun, Bandgap-like strong fluorescence in functionalized carbon nanoparticles, *Angew.*
 409 *Chem. Int. Ed.* 49 (2010) 5310–5314. <https://doi.org/10.1002/anie.201000982>.

410 [22] P. Anilkumar, X. Wang, L. Cao, S. Sahu, J.-H. Liu, P. Wang, K. Korch, K.N. Tackett II,
 411 A. Parenzan and Y.-P. Sun, Toward quantitatively fluorescent carbon-based “quantum” dots.
 412 *Nanoscale*. 3 (2011) 2023–2027.

413 [23] C. Jiang, H. Wu, X. Song, X. Ma, J. Wang, M. Tan, Presence of photoluminescent
 414 carbon dots in Nescafe® original instant coffee: applications to bioimaging, *Talanta*. 127
 415 (2014) 68–74. <https://doi.org/10.1016/j.talanta.2014.01.046>.

416 [24] F. Arcudi, L. Đorđević, M. Prato, Synthesis, separation, and characterization of small and
 417 highly fluorescent nitrogen-doped carbon nanodots, *Angew. Chem. Int. Ed.* 55 (2016) 2107–
 418 2112. <https://doi.org/10.1002/anie.201510158>.

419 [25] A.A. Kokorina, E.S. Prikhozhenko, N.V. Tarakina, A.V. Sapelkin, G.B. Sukhorukov,
 420 I.Y. Goryacheva, Dispersion of optical and structural properties in gel column separated
 421 carbon nanoparticles, *Carbon*. 127 (2018) 541–547.
 422 <https://doi.org/10.1016/j.carbon.2017.11.039>.

423 [26] N. Fuyuno, D. Kozawa, Y. Miyauchi, S. Mouri, R. Kitaura, H. Shinohara, T. Yasuda, N.
 424 Komatsu, K. Matsuda, Drastic change in photoluminescence properties of graphene quantum
 425 dots by chromatographic separation. *Adv. Opt. Mater.* 2 (2014) 983–989.
 426 <https://doi.org/10.1002/adom.201400200>.

427 [27] R. Ye, C. Xiang, J. Lin, Z. Peng, K. Huang, Z. Yan, N.P. Cook, E.L.G. Samuel, C.-C.
 428 Hwang, G. Ruan, G. Ceriotti, A.-R.O. Raji, A.A. Marti, J.M. Tour, 2013. Coal as an abundant
 429 source of graphene quantum dots. *Nat. Commun.* 4, 2943.
 430 <https://doi.org/10.1038/ncomms3943>.

431 [28] S. Ciftan Hens, W.G. Lawrence, A.S. Kumbhar, O. Shenderova, Photoluminescent
 432 nanostructures from graphite oxidation, *J. Phys. Chem. C*. 116 (2012) 20015–20022.
 433 <https://doi.org/10.1021/jp303061e>.

434 [29] K.A. Laptinskiy, S.A. Burikov, S.V. Patsaeva, I.I. Vlasov, O.A. Shenderova, T.A.
 435 Dolenko, 2020. Absolute luminescence quantum yield for nanosized carbon particles in water
 436 as a function of excitation wavelength. *Spectrochim. Acta A*. 229, 117879.
 437 <https://doi.org/10.1016/j.saa.2019.117879>.

438 [30] O.E. Trubetskaya, C. Richard, S.V. Patsaeva, O.A. Trubetskoj, 2020. Evaluation of
 439 aliphatic/aromatic compounds and fluorophores in dissolved organic matter of contrasting
 440 natural waters by SEC-HPLC with multi-wavelength absorbance and fluorescence detections.
 441 *Spectrochim. Acta A*. 238, 118450. <https://doi.org/10.1016/j.saa.2020.118450>.

442 [31] O.A. Trubetskoj, C. Richard, G. Voyard, V.V. Marchenkov, O.E. Trubetskaya,
 443 Molecular size distribution of fluorophores in aquatic natural organic matter: application of
 444 HPSEC with multi-wavelength absorption and fluorescence detection following LPSEC-
 445 PAGE fractionation, *Environ. Sci. Technol.* 52 (2018) 5287–5295.
 446 <https://doi.org/10.1021/acs.est.7b03924>.

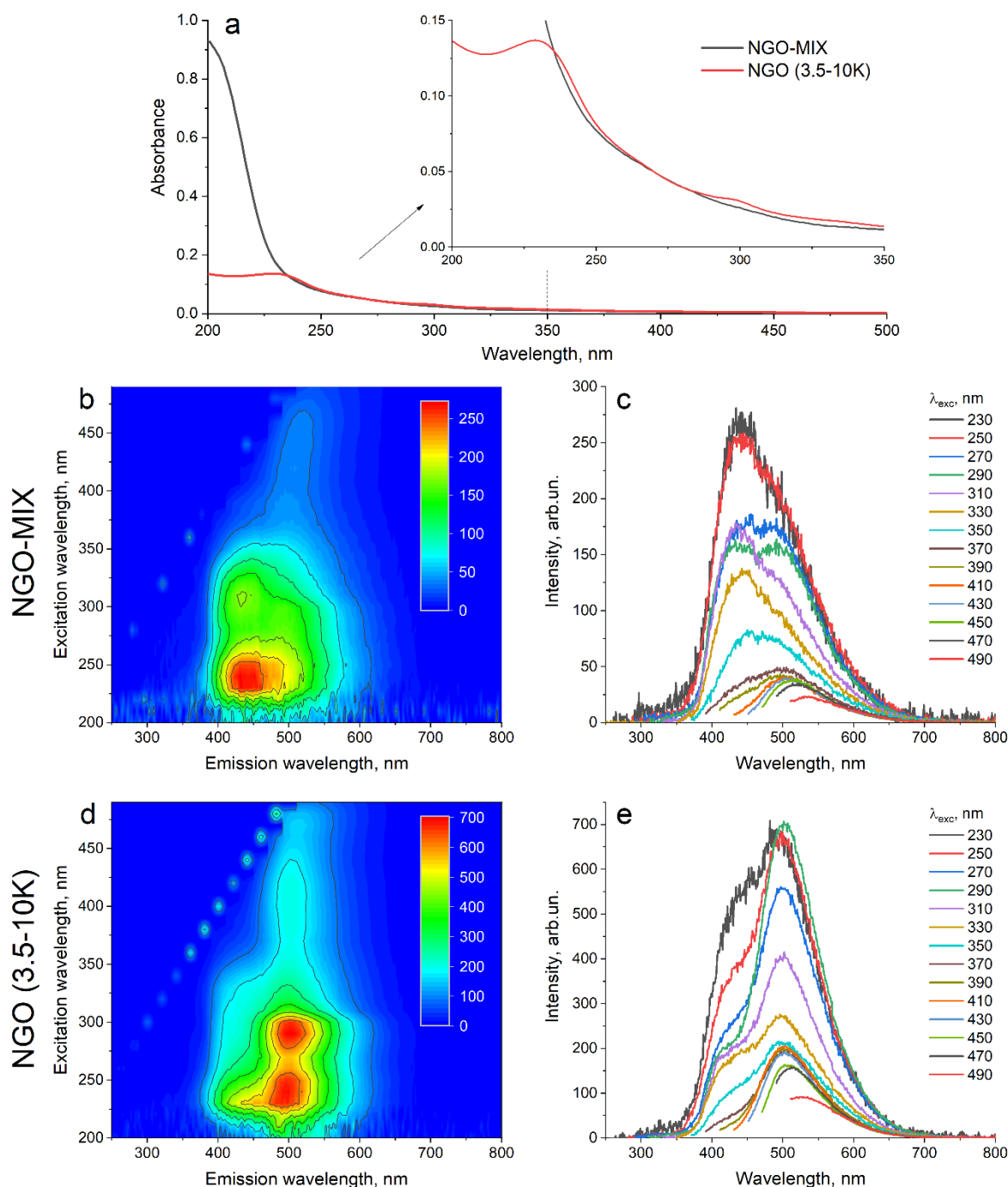


Figure 1. The absorbance spectra of NGO-MIX and NGO (3.5-10K) samples (a). The EEM of NGO-MIX (b) and NGO (3.5-10K) (d), the sets of conventional emission spectra of NGO-MIX (c) and NGO (3.5-10K) (e). The absorbance and fluorescence spectra were recorded for NGO aqueous solutions with absorption of 0.05 at 270 nm.

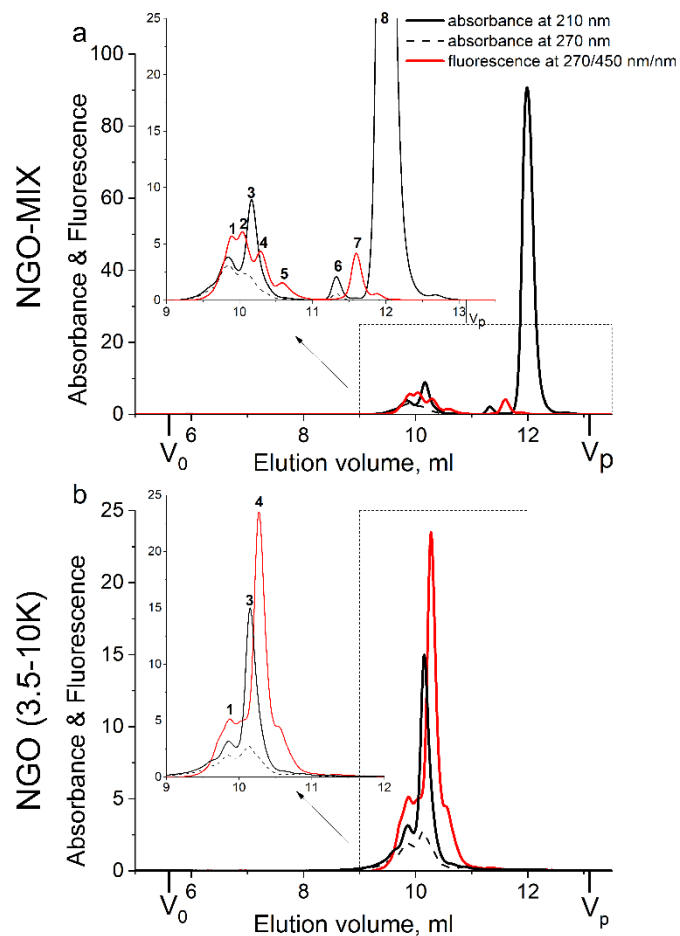


Figure 2. HPSEC chromatograms of NGO-MIX (a) and NGO (3.5-10K) (b) on TSKgel G2000SW_{XL} column in 30 mM phosphate buffer (pH 6.5) with absorbance detections (at 210 nm, solid black lines, and at 270 nm, dashed black lines) and fluorescence detection (at $\lambda_{\text{exc}}/\lambda_{\text{em}} = 270/450$ nm/nm, solid red lines).

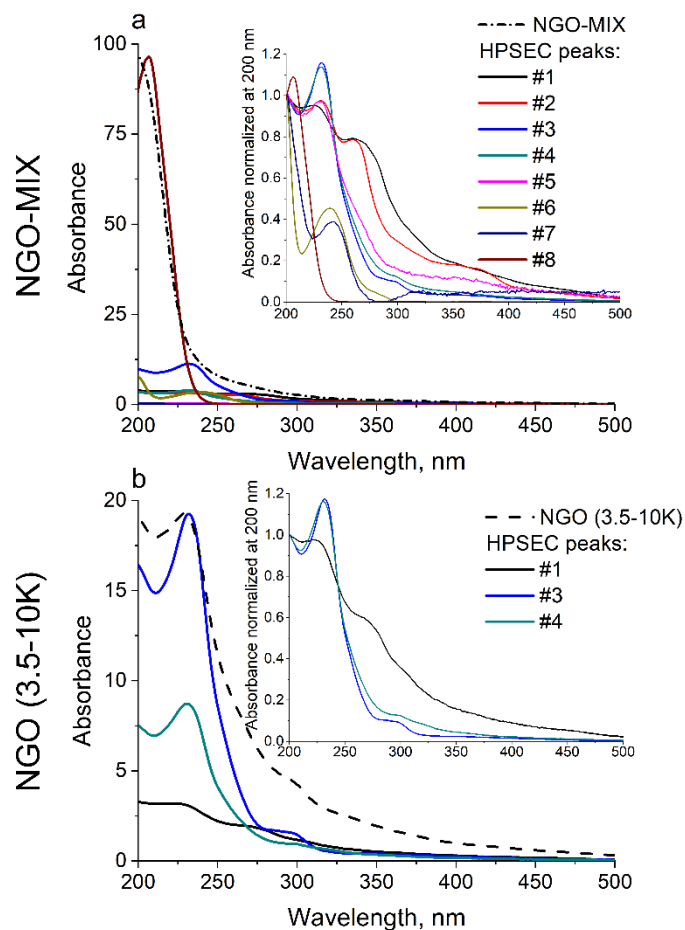


Figure 3. Absorbance spectra of NGO-MIX and its HPSEC peaks #1-#8 (a), of NGO (3.5-10K) and its HPSEC peaks #1, #3, and #4 (b). *Insets:* normalized at 200 nm absorbance spectra of NGO-MIX peaks #1-#8 (a) and NGO (3.5-10K) peaks #1, #3, and #4 (b).

464 **Table 1.** Elution volumes (V_e) and absorbance maxima in UV-vis region of the bulk NGO-
 465 MIX, NGO (3.5-10K) and HPSEC peaks. The absorbance spectra were extracted from the
 466 data of the multi-wavelength absorbance detector at V_e corresponded to the chromatographic
 467 peaks' tops.

Peak number	V_e , ml	Absorbance maxima, nm	
		NGO-MIX	NGO (3.5-10K)
Bulk sample	-	No max	228 sh*300
1	9.89	224 260	221 sh 270
2	10.03	231 260 sh 365	-
3	10.15	232 sh 290 sh 365	232 sh 290
4	10.29	230 sh 300	230 sh 300
5	10.59	230 sh 260 sh 350	-
6	11.31	238 sh 280	-
7	11.59	242 320	-
8	12.00	206	-

468
 469

*sh– shoulder